Transactions on Computer Science and Intelligent Systems Research
ISSN: 2960-1800, eISSN: 2960-2238 | Volume 11
TPCEE 2025

Lens-Free Microscopic Imaging for 3D Analysis of Insect Microstructures and Ecological Applications

Yangxiao (Olivia) Ou *

Fayetteville High School, Fayetteville, United States of America

* Corresponding Author Email: oliviaou2007@gmail.com

Abstract. Traditional microscopes provide only 2D intensity information for transparent or unstained samples, limiting access to 3D morphology. Here, we present an in-line lensless digital holographic system using a 532 nm monochromatic light source. The unmodulated direct component serves as the reference wave, and the sample-diffracted component forms the interference, enabling single-frame 3D reconstruction via angular spectrum analysis. The system integrates a board-level CMOS camera with a simplified optical-mechanical structure, alongside automated preprocessing, conjugate suppression, and phase unwrapping. Unified sampling and coherence constraints yield a well-defined effective FOV, allowing quantitative 3D imaging of butterfly antennae and earthworm cross-sections. This low-cost, portable approach bypasses the need for expensive objectives and complex calibration, complementing—but not replacing—high-end instruments. Current limitations include axial calibration and phase noise control; future work will incorporate multi-frame phase shifting, learning-based conjugate suppression, and reflective imaging for strongly scattering samples. This platform provides accessible 3D imaging for entomology, biophotonics, biomimetic materials, and optical device research.

Keywords: Digital Holography; Interferometric Measurement; Three-Dimensional Imaging.

1. Introduction

Global climate change is rapidly reshaping ecosystems by altering temperature, humidity, CO_2, and extreme weather patterns, which in turn affect insect body size, cuticle hardening, and water content. As vital agents in pollination and decomposition, insects also serve as sensitive indicators of disturbance. Thus, quantitative, long-term, and non-invasive imaging methods are essential for studying their microstructural dynamics under near-natural conditions.

Conventional optical microscopy (brightfield, phase contrast, DIC) remains widely used but suffers from key limitations: (1) loss of axial information due to 2D projection; (2) disturbance from fixation or staining; (3) poor reproducibility across laboratories; and (4) insufficient capacity for continuous long-term tracking. As a result, structural adaptations to climate stress—such as wing membrane thickening or spiracle displacement—remain difficult to monitor.

Digital holographic microscopy (DHM) provides a solution by recording interference patterns and enabling quantitative 3D reconstruction. Since Gabor's introduction of holography in 1948 [1], followed by Leith and Upatnieks' use of lasers in the 1960s [2], and the integration of CMOS sensors and Fourier algorithms in the 1980s [3–5], DHM has matured into a powerful imaging technique. Compared with SEM and confocal microscopy, lens-less DHM uniquely enables real-time, non-destructive, and cost-effective monitoring of live insect microstructures (Table 1).

Table 1. Performance Comparison of Four Microscopy Techniques

Parameter	Optical Microscope (Olympus BX53)	Electron Microscope (JEOL JSM-IT200 SEM)	Confocal Microscope (Leica TCS SP8)	Lens-less Digital Holographic Microscopy (Our System)
3D Measurement	2D imaging only	Surface topology, requires vacuum and conductive coating	Optical sectioning enables 3D reconstruction	Holographic reconstruction provides full 3D information
Lateral Resolution	~200 nm (diffraction-limited)	~1–2 nm (ultra-high resolution)	~180 nm (better than conventional optical)	~2 μm (limited by pixel size and reconstruction algorithm)
Field of View (20×)	~1 mm × 1 mm	~50 μm × 50 μm	~0.5 mm × 0.5 mm	33.18mm²
Cost Range	~$20,000–$50,000	~$500,000–$1,000,000	~$250,000–$600,000	<$500 (CMOS/LED-based, low-cost)
Ease of Use	Simple operation, widely available	Complex sample prep, requires skilled operators	Requires labeling and precise calibration	Simple setup, reconstruction handled by algorithms
Size / Weight	Medium, desktop size	Large, several hundred kilograms	Large, requires dedicated lab space	Small, portable, can be implemented in handheld format
Full-field Measurement Time	Real-time (video-rate)	Slow (point-by-point scanning, several minutes)	Moderate (layer-by-layer scanning, tens of seconds to minutes)	Real-time (single exposure + fast computational reconstruction)

Figure 1. (a)Optical Microscope (Olympus BX53) (b) Electron Microscope (JEOL JSM-IT200 SEM) (c) Confocal Microscope (Leica TCS SP8)

Our study develops a simplified DHM system for insect antennae characterization. Using a green monochromatic light source and a 2 μm CMOS camera, the setup eliminates lenses while retaining reliable 3D reconstruction. Automated MATLAB algorithms streamline acquisition, aberration correction, and dynamic tracking, balancing simplicity with accuracy. This approach establishes a practical methodology for linking insect microstructures with climate-driven morphological change, while expanding the accessibility of holographic imaging across ecological and biomimetic applications.

The rest of this paper if structured as follows: Section 1: Basic principle of DHM, it focus on the principles of interference recording and diffraction reconstruction. Section 2: Optical path design. Section 3: Hardware setup. Section 4: sample measuring. Section 5: conclusion of this paper. Section 6: Reference.

2. Basic Principle of Digital Holographic Microscopy

Digital holographic microscopy (DHM) enables quantitative 3D measurement of microscopic morphology by reconstructing both amplitude and phase. Compared with conventional microscopy, it provides non-invasive, full-field imaging with high phase sensitivity. In this study, an in-line DHM system with a 532 nm green source and a 2 μm pixel Basler CMOS camera was used. The in-line (Gabor) design offers a simple optical path and efficient spatial bandwidth but requires conjugate image separation [6]. Diffraction reconstruction employed the angular spectrum method, achieving nanoscale phase accuracy through frequency-domain processing.

2.1. Mechanism of Interference Field Formation

Digital holographic microscopy (DHM) records the interference between object and reference waves to encode 3D information. When coherent monochromatic light illuminates a weakly scattering sample, the field consists of two parts [7]:

a. Reference wave: undisturbed plane wave:

$$R(x,y)=A_R e^{i\phi_R} \tag{1}$$

b. Object wave: carries structural information via amplitude attenuation and phase delay:

$$O(x,y)=A_O(x,y)e^{i\phi_O(x,y)} \tag{2}$$

Unlike conventional interferometers, self-interference occurs naturally, forming an intensity pattern on the detector.

2.2. Principles of In-line Holographic Encoding and Frequency-domain Analysis

In in-line DHM, object and reference waves share the optical axis (Gabor geometry) [8]. The recorded intensity is:

$$I(x,y)=|R(x,y)+O(x,y)|^2=|R|^2+|O|^2+R^*O+RO^* \tag{3}$$

Where, $|R|^2$ and $|O|^2$ are DC terms, while R*O and RO*encode conjugate-symmetric information.

Key features:

- Spectral overlap of $O(f_x,f_y)$ and $O^*(-f_x,-f_y)$;
- Doubled theoretical cutoff frequency, $f_{max}=1/(2\Delta x)$;
- Need for phase-shifting/iterative separation.

The Fourier spectrum shows center symmetry due to conjugate overlap:

$$FI_H=|R|^2\delta(0,0)+F|O|^2+O(f_x,f_y)+O^*(-f_x,-f_y) \tag{4}$$

2.3. Principle of Diffraction Reconstruction

Reconstruction numerically simulates wave propagation based on scalar diffraction theory [9]. Treating the hologram as a diffraction screen, the angular spectrum method computes field propagation as

$$U(x,y;d)=F^{-1}\left\{F[I_H]\cdot \exp\left(\frac{i2\pi d}{\lambda}\sqrt{1-(\lambda f_x)^2-(\lambda f_y)^2}\right)\right\} \tag{5}$$

Steps:

Fourier transform of hologram:

$$F(f_x,f_y)=FFT[I_H(x,y)] \tag{6}$$

1. Multiply by transfer function:

$$F'(f_x,f_y)=F(f_x,f_y)\cdot \exp\left(i\frac{2\pi d}{\lambda}\sqrt{1-(\lambda f_x)^2-(\lambda f_y)^2}\right) \tag{7}$$

2. Inverse FFT to reconstruct:

$$U(x,y)=IFFT[F'(f_x,f_y)] \tag{8}$$

3. Optical Path Design

The digital holographic microscopy system in this study adopts a modular design, with each optical element precisely positioned and mechanically stabilized using custom 3D-printed fixtures. This architecture ensures flexible assembly, accurate alignment, and reproducible performance, providing the foundation for the overall system configuration.

3.1. System Hardware Architecture

The system comprises an optical frame, imaging module, light source, and sample holder. The support frame, fabricated from lightweight PLA, maintains in-line alignment of all components within ±0.1 mm tolerance [10], a prerequisite for high-quality interference and reconstruction. At the base, a Basler board-level camera (2 cm × 2 cm) captures interference fringes with high SNR. A 532 nm monochromatic laser, mounted above, balances illumination intensity and biological specimen safety [11]. An overview of the setup is shown in Figure 2.

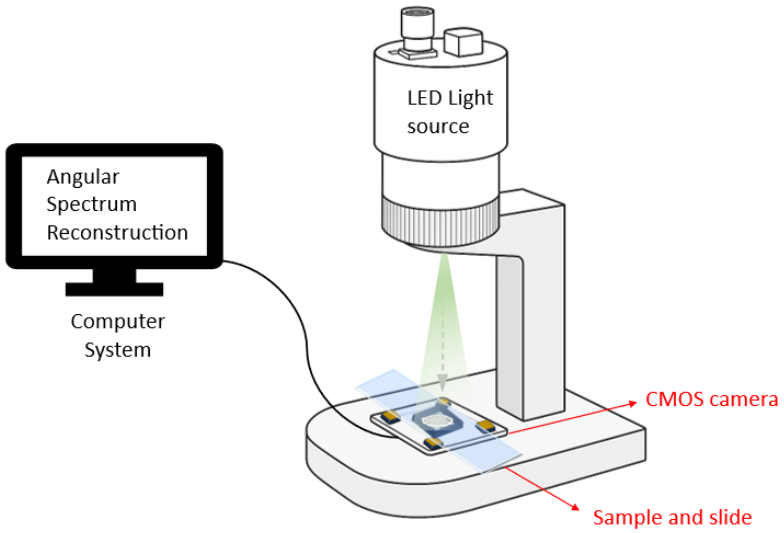

Figure 2. Overview of the system.

The sample holder, located directly above the sensor, employs glass slides and is restricted to transmissive specimens (e.g., thin slices, transparent microstructures). Transparency is essential, as excessive absorption or scattering compromises object-wave integrity, hologram contrast, and reconstruction fidelity [12].

The source-to-sample distance is optimized between 7–10 cm. Distances below 7 cm narrow the interference region and risk edge information loss, while distances above 10 cm attenuate intensity and degrade fringe visibility. The chosen range provides a balance between field coverage and stability, ensuring robust holographic recording.

3.2. Image Reconstruction and Advantages of Lens-Free Imaging Architecture

The system implements image reconstruction on MATLAB. Recorded holograms are Fourier-transformed to separate object and reference waves, eliminating zero-order diffraction and conjugate interference. Phase unwrapping, combined with the Fresnel diffraction model, converts 2D intensity data into a 3D representation for detailed structural visualization [13]. The following prosses illustrate the process of the software imaging:

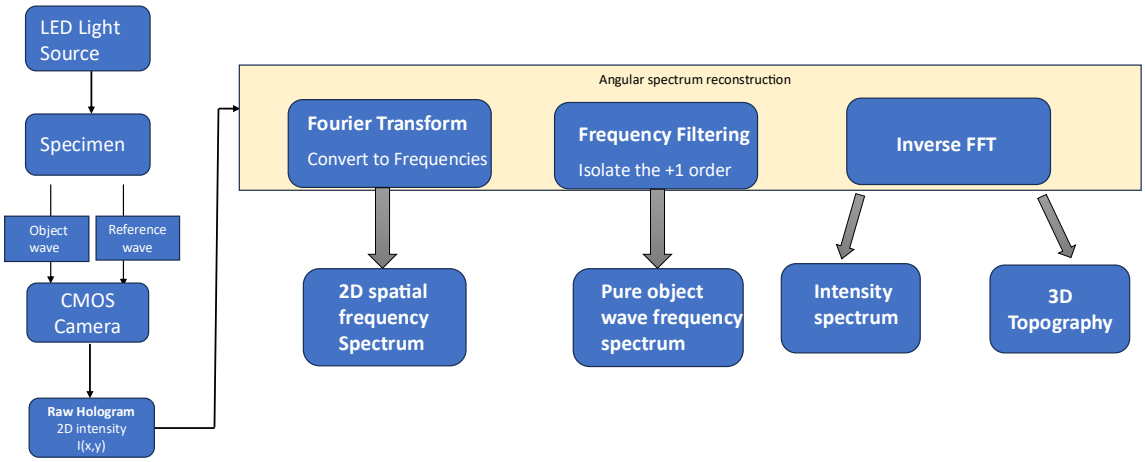

Figure 3. The workflow of the system.

Compared with conventional microscopy, the lens-free architecture offers key advantages:

Aberration-Free Imaging: Digital holographic reconstruction compensates for phase errors accumulated during propagation, mitigating optical aberrations such as spherical or chromatic distortion that affect high-magnification objectives [14].

Wide Field of View with High Resolution: By adjusting the source-sample distance, the system achieves ~2 μm lateral resolution and a maximized FOV determined by the CMOS sensor:

$$N_x \times \Delta x \times N_y \times \Delta y = 3840 \times 2\ \mu m \times 2160 \times 2\ \mu m = 33.18\ mm^2 \tag{9}$$

3.3. Rationale for Key Component Selection

3.3.1. Selection of the Green Monochromatic Light Source.

A 532 nm green laser was selected for three reasons: (1) Resolution: shorter wavelength improves lateral resolution according to Rayleigh criterion ($\sigma=0.61\lambda/NA$), and 532 nm offers stable intensity over short propagation distances, enhancing interference quality; (2) Sample Compatibility: low absorption by biological specimens minimizes photodamage and reduces air-induced noise; (3) Camera Matching: the Basler sensor has optimal spectral response at 500–600 nm, ensuring high SNR for weak interference signals.

3.3.2. Camera Selection.

A 2 μm × 2 μm pixel camera was chosen to match sample feature size (~2 μm, e.g., butterfly antennae), balancing sufficient structural resolution with manageable data volume and computational efficiency during MATLAB reconstruction. Higher-resolution cameras would increase pixel count and computation time without significantly improving imaging quality.

3.3.3. Selection of Transmissive Samples.

Transmissive samples are essential to generate interference fringes and preserve phase information. They allow the object wave to encode internal structural variations, minimize scattering, and maintain strong signal intensity. Opaque samples would block or reflect the object wave, preventing hologram formation and reducing reconstruction fidelity.

3.4. Summary

Table 2. System Parameters of the Lens-less Digital Holographic Microscopy System

Parameter	Symbol	Optimized Value	Theoretical Basis
Source-to-sample distance	d_1	7–10 cm	Ensures uniform illumination: $d_1 > D^2/\lambda$ (where D is the beam diameter)
Sample-to-detector distance	d_2	450–1000 μm	Satisfies Fresnel condition: $d_2 > (N\Delta x)^2/\lambda$
Spatial resolution	δ	2.0 μm	Sample microstructures are separated by distances greater than 2 μm
Field of view	FOV	33.18 mm²	FOV=$N_x \Delta x \times N_y \Delta y$

4. Hardware Setup

The system adopts a modular architecture with a Basler daA3840-45um monochrome CMOS camera [Fig. 4(a)] and a Daheng Optics GCI-060403 green LED [Fig. 4(b)] to ensure high spatial sampling and interference contrast while minimizing speckle. The optical-mechanical assembly consists of a 3D-printed PLA frame (~140 mm height) [Fig. 4(c)] with a plastic spacer fixing the light source–sample distance at 90 mm. Samples are placed on the CMOS protective glass, with adjustable sample–camera distance d_2 of 450–1000 μm, yielding lateral resolution of 3.2–1.8 μm per Fresnel diffraction. The camera is initialized via Pylon Viewer, and the LED is aligned to the optical axis within ±0.1

mm. Transparent slides serve as sample holders, and measurements are performed in a dark environment with source intensity adjusted through the Pylon Viewer.

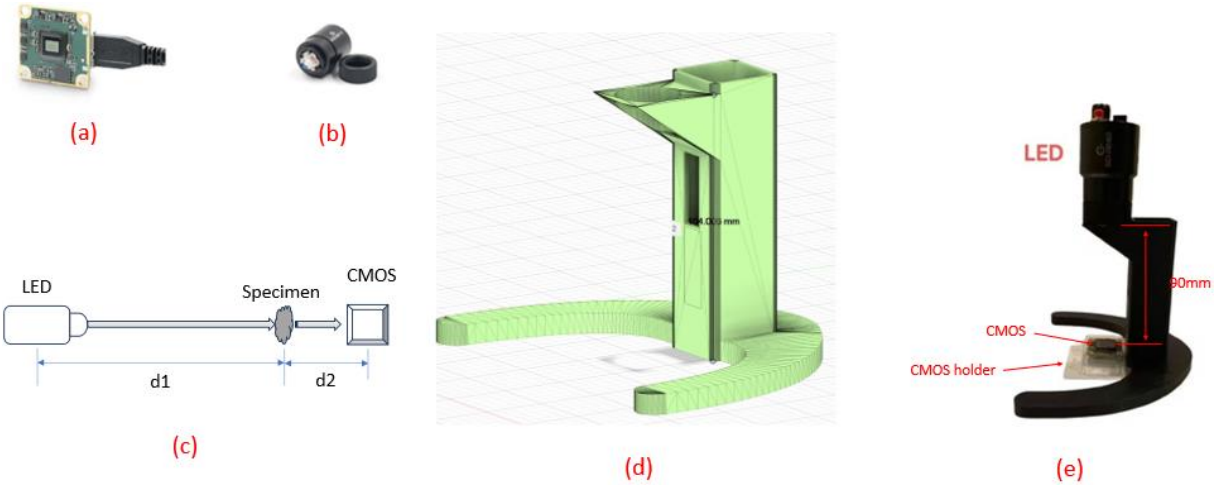

Figure 4. System structure diagram

5. Sample Measuring

To validate 3D imaging, butterfly antennae (including tips) and earthworm cross-sections were reconstructed. High-precision imaging captured microstructural spatial features, providing direct morphological data to support further studies. Measurement results are shown below:

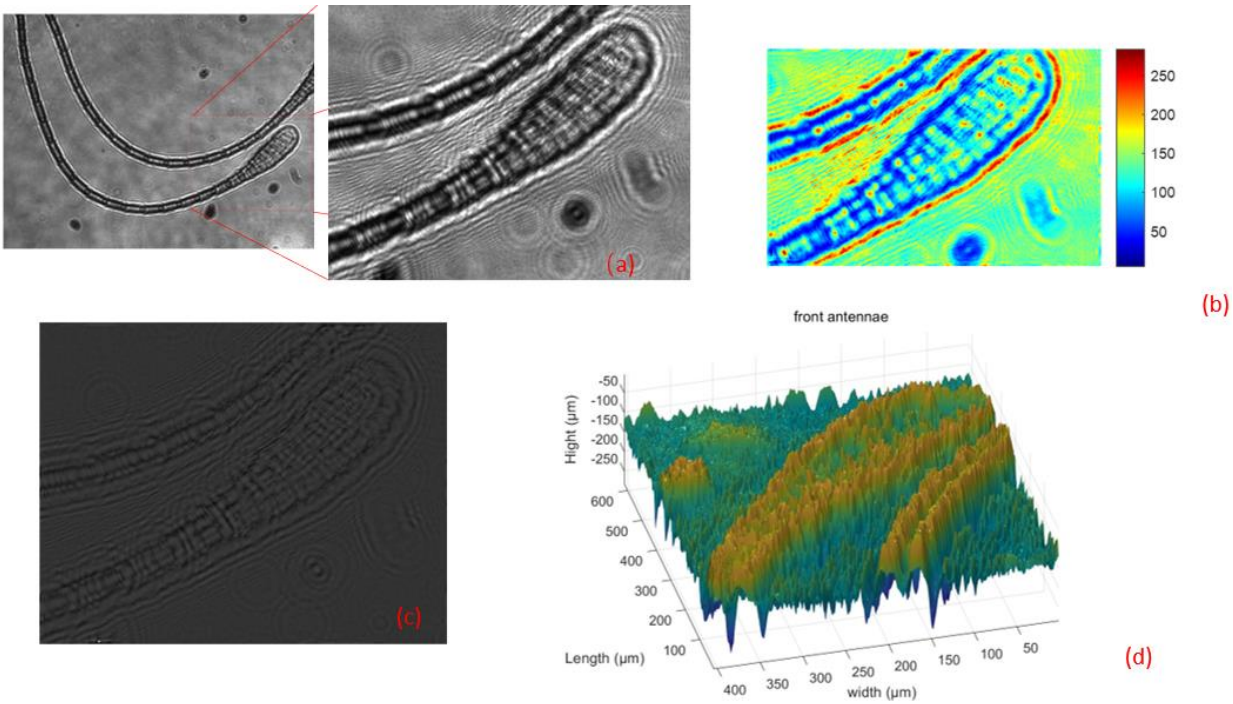

Figure 5. Three-dimensional measurement results of butterfly antennae

The system resolves 3D structural details of butterfly antenna tips beyond traditional circular cross-sections. Figure 5 shows (a) the captured hologram, (b) intensity map with color bar (0–250) for quantitative analysis, (c) phase distribution, and (d) 3D reconstruction via phase unwrapping. Numerical differences between main body (50–100) and fine edges (150–200) reflect structural heterogeneity. These results demonstrate the system's capability to reveal morphological features and functional information inaccessible to conventional 2D microscopy, providing an advanced tool for studying insect cuticle structure and its responses to environmental changes.

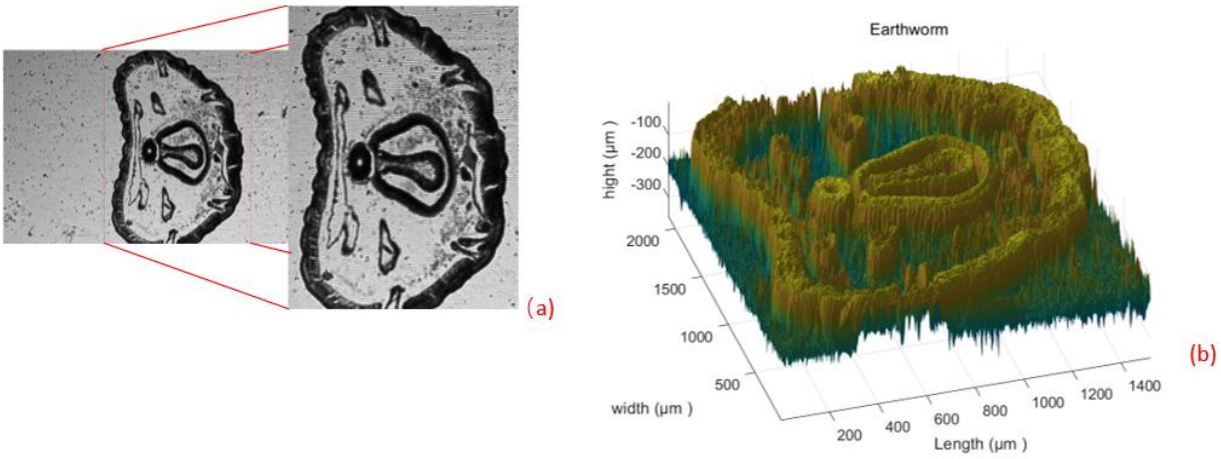

Figure 6. Earthworm cross-sections

In observations of earthworm cross-sections, 2D images (a) show overall contours and major internal structures, providing a basic morphological overview but only surface gray-scale differences, limiting axial information. In contrast, 3D reconstruction (b) captures spatial undulations, longitudinal height, and thickness variations, providing quantitative structural data. This enhanced 3D information allows objective analysis of tissue mechanics and functional adaptations, highlighting the system's advantage for complex biological samples.

6. Conclusion

This imaging system integrates holographic imaging, phase analysis, and 3D reconstruction, providing a complete workflow from data acquisition to multi-dimensional analysis. High-precision cameras combined with custom optical components capture high-quality holograms, while dedicated algorithms enable efficient hologram decoding, phase unwrapping, and 3D modeling.

The system is cost-effective, user-friendly, and capable of multi-dimensional imaging, generating holograms, color maps, phase maps, and 3D reconstructions. For example, imaging butterfly antennae reveals both surface optical properties and detailed 3D morphology. The in-line Gabor configuration simplifies alignment, ensures uniform fringe distribution, and enhances the fidelity and efficiency of holographic reconstruction. This enables intuitive visualization of insect microstructures, facilitating analysis of structural-functional relationships and offering practical tools for research in entomology, botany, and zoology.

The primary limitation of this study is the absence of a resolution plate to experimentally test the system's lateral and axial resolution, preventing precise quantification of the imaging performance.

Acknowledgements

This is the place to fill in information about funds, sponsors, etc. that need to be thanked.

References

[1] Gabor, D. "Holography, 1948-1971." Science, vol. 177, no. 4046, 28 July 1972, pp. 299 – 313, science.sciencemag.org/content/177/4046/299, https://doi.org/10.1126/science.177.4046.299.

[2] Leith, Emmett N., and Juris Upatnieks. "Wavefront Reconstruction with Diffused Illumination and Three-Dimensional Objects*." Journal of the Optical Society of America, vol. 54, no. 11, 1 Nov. 1964, p. 1295, https://doi.org/10.1364/josa.54.001295. Accessed 2 Mar. 2023.

[3] Colomb, Tristan, et al. "Advantages of digital holographic microscopy for real-time full field absolute phase imaging." Three-Dimensional and Multidimensional Microscopy: Image Acquisition and Processing XV. Vol. 6861. SPIE, 2008.

[4] Hayes-Rounds, Charity, et al. "Advantages of Fresnel biprism-based digital holographic microscopy in quantitative phase imaging." Journal of biomedical optics 25.8 (2020): 086501 - 086501.

[5] Zhang, Jialin, et al. “Resolution Analysis in a Lens-Free On-Chip Digital Holographic Microscope.” IEEE Transactions on Computational Imaging, vol. 6, Jan. 2020, pp. 697 – 710. https://doi.org/10.1109/tci.2020.2964247.

[6] Latychevskaia, Tatiana, et al. "Off-axis and inline electron holography: Experimental comparison." Ultramicroscopy 110.5 (2010): 472 - 482.

[7] Kim, Myung K. "Principles and techniques of digital holographic microscopy." SPIE reviews 1.1 (2010): 018005.

[8] Huang, Zhengzhong, and Liangcai Cao. “Quantitative Phase Imaging Based on Holography: Trends and New Perspectives.” Light Science & Applications, vol.13, no.1, June 2024, https://doi.org/10.1038/s41377 - 024 - 01453 - x.

[9] Guangjun, Wang, et al. “Comparison of Commonly Used Numerical Reconstruction Algorithms in Digital Holographic Microscopy.” Laser & Optoelectronics Progress, vol. 47, no. 3, Jan. 2010, p. 030901. https://doi.org/10.3788/lop47.030901.

[10] Zhang, Jiwei, et al. “A Review of Common-path Off-axis Digital Holography: Towards High Stable Optical Instrument Manufacturing.” Light Advanced Manufacturing, vol.2, no.3, Jan.2021, p.1. https://doi.org/10.37188/lam.2021.023.

[11] Kozacki, Tomasz, and Maksymilian Chlipala. "Color holographic display with white light LED source and single phase only SLM." Optics Express 24.3 (2016): 2189 - 2199.